

Towards Pragmatic Semantic Image Synthesis for Urban Scenes

George Eskandar^{1*}, Diandian Guo^{*1}, Karim Guirguis², Bin Yang¹

¹Institute of Signal Processing and System Theory, University of Stuttgart, Stuttgart, Germany

²Bosch Center for Artificial Intelligence, Renningen, Germany

Abstract—The need for large amounts of training and validation data is a huge concern in scaling AI algorithms for autonomous driving. Semantic Image Synthesis (SIS), or label-to-image translation, promises to address this issue by translating semantic layouts to images, providing a controllable generation of photorealistic data. However, they require a large amount of paired data, incurring extra costs. In this work, we present a new task: given a dataset with synthetic images and labels and a dataset with unlabeled real images, our goal is to learn a model that can generate images with the content of the input mask and the appearance of real images. This new task reframes the well-known unsupervised SIS task in a more practical setting, where we leverage cheaply available synthetic data from a driving simulator to learn how to generate photorealistic images of urban scenes. This stands in contrast to previous works, which assume that labels and images come from the same domain but are unpaired during training. We find that previous unsupervised works underperform on this task, as they do not handle distribution shifts between two different domains. To bypass these problems, we propose a novel framework with two main contributions. First, we leverage the synthetic image as a guide to the content of the generated image by penalizing the difference between their high-level features on a patch level. Second, in contrast to previous works which employ one discriminator that overfits the target domain semantic distribution, we employ a discriminator for the whole image and multiscale discriminators on the image patches. Extensive comparisons on the benchmarks GTA-V → Cityscapes and GTA-V → Mapillary show the superior performance of the proposed model against state-of-the-art on this task.

Index Terms—GANs, Image-to-Image Translation, Semantic Image Synthesis, Synthetic Data, Unsupervised Learning

I. INTRODUCTION

Semantic Image Synthesis is a subclass of Image-to-Image translation (I2I) where an image is generated from a semantic layout. In the context of autonomous driving, SIS is a promising method for generating diverse training and validation data because it can provide photorealism and controllability, two essential qualities for data augmentation schemes. Photorealism means that the generated images have the same texture and appearance as images recorded in real life; otherwise, a domain gap will ensue from the difference between training and test time distributions. On the other hand, controllability

* Both authors equally contributed to this work

Corresponding author email: george.eskandar@iss.uni-stuttgart.de

The research leading to these results is funded by the German Federal Ministry for Economic Affairs and Energy within the project "AI Delta Learning." The authors would like to thank the consortium for the successful cooperation.

Code is available at <https://github.com/GeorgeEskandar/Towards-Pragmatic-Semantic-Image-Synthesis-for-Urban-Scenes>

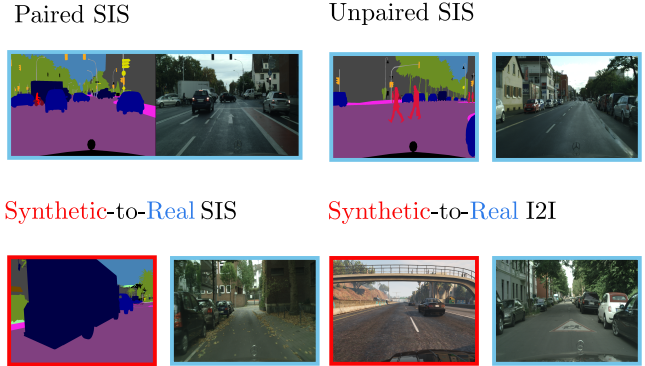


Fig. 1: Overview of different SIS and I2I paradigms: (a) Paired SIS, (b) Unpaired SIS: the common setting in the previous works was to assume images and labels come from the same distribution but they are unpaired, (c) Synthetic-to-Real SIS: the proposed task, labels come from a synthetic data, images originate from a real dataset, (d) Synthetic-to-Real I2I: source and target domains are different, but images are used in both domains, which is considerably easier than using labels as input, but does not provide controllability.

Task	Photorealism	Controllability	Cross-Domain	Cheap data
Syn-to-Real I2I	✓	✗	✓	✓
Paired SIS	✓	✓	✗	✗
Unpaired SIS	✓	✓	✗	✗
Syn-to-Real SIS	✓	✓	✓	✓

TABLE I: Comparison between different SIS and I2I paradigms: the proposed task combines several practical advantages compared to the previous tasks.

means that the user can generate or edit an image with predefined characteristics (changing weather, adding or removing cars, changing road width, increasing the number of pedestrians ...). Having user control over the input RGB space is of special interest for model validation [1] because it helps understand an AI model's decision through counterfactual reasoning: for instance, we wish to know whether a perception algorithm would behave correctly had there been more cars or pedestrians in a given scene. In this regard, SIS allows easy and explicit user control of scene editing through the manipulation of the input semantic map. For instance, one can add, delete or alter the style of different objects. SIS has been pivotal in several frameworks [2–4] where semantic layouts are used as a prior for urban scene generation.

However, the necessity for a significant amount of paired

training data undermines the initial intent of SIS, which was to provide inexpensive data augmentation. Unsupervised approaches [5–16] have shown impressive results without needing paired data, but because they rely on ideal assumptions, their usefulness in the actual world is limited. Mainly, they employ paired datasets (like Cityscapes) and present the images and labels to the model in an unpaired way in each training iteration mimicking a real unpaired setting. This has brought us to ask the following questions: *what would a truly unpaired training setting for SIS look like? and how to pragmatically collect cheap semantic layouts for training?*

In this work, we propose a new task, Synthetic-to-Real SIS, where a mapping is learned from a set of synthetic labels to a set of real images (Figure 1). Since labels and images originate from 2 different domains, not only is the setting truly unpaired but also pragmatic because producing semantic layouts from a driving simulator [17], or a graphics engine [18] is inexpensive (Table I). However, this task also introduces a new challenge: it is almost inevitable that the source and target datasets (labels and images, respectively) will have different class distributions. For instance, the synthetic dataset might contain a large proportion of buildings, while the real dataset has fewer buildings and more trees. Cross-domain differences could potentially lead to undesired semantic misalignments in the generated images (such as generating trees instead of buildings) because the model tries to imitate the target domain and ignores the source label map. This would undermine the utility of unpaired generative models.

We show that unpaired GANs underperform on the Synthetic-to-Real SIS task, as they ignore cross-domain semantic mismatches. To this end, we introduce a new framework that bypasses this limitation. The key idea of our framework is to learn to generate an image with the appearance of real images but with the content of the synthetic image that corresponds to the input label. In other words, we use the synthetic image as a *guide* to the content of the generated image by leveraging high-level features of a pre-trained network. Our contributions can be summarized as follows: (1) We propose Synthetic-to-Real SIS, a new task that allows training an SIS model in a pragmatic and low-cost way, (2) we develop a new framework for this task that exploits the similarity between generated and synthetic *patches* to preserve alignment with the input layout, and (3) in contrast to previous works which use one discriminator, we employ multiple discriminators on both the *global* and *local* image contexts to prevent overfitting on simple visual cues in the target domain. Experiments on 2 benchmarks, GTA-V → Cityscapes and GTA-V → Mapillary, show the superior performance of our model compared to state-of-the-art approaches.

II. RELATED WORKS

Semantic image synthesis is the task of translating semantic layouts to images [19]. In contrast to I2I [20], SIS is a severely under-constrained task because the input layout has fewer details than the output image, which is rich in high spatial

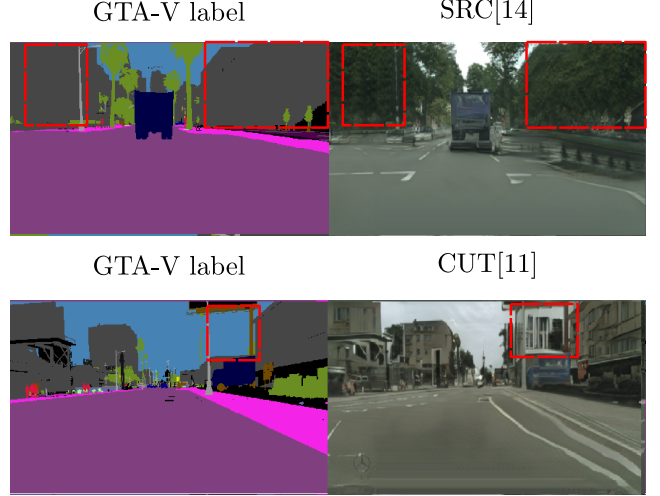


Fig. 2: Performance of state-of-the-art unpaired models on Synthetic-to-Real USIS. Semantic inconsistencies (in red) can appear between the label and images.

frequencies like edges, corners, and texture. SPADE [21] has made a breakthrough in this task by designing spatially adaptive normalization layers. Since then, a plethora of frameworks [22–26] has presented progressive architectural improvements to enhance the fidelity and alignment of generated images.

Unpaired image-to-image translation is the translation of one image collection (source domain) to another (called target domain). There have been 2 main approaches to unpaired I2I: cycle consistency losses [5–7] and relationship preservation constraint [8–14]. In our previous work, we designed a framework, USIS [15, 16], that achieves state-of-the-art results on the unpaired label-to-image translation task. In this work, we try to extend USIS to a more realistic unpaired scenario for urban scene generation.

Synthetic to real translation is one application of unpaired I2I, where a synthetic image (produced from a simulation environment) is translated to a photorealistic image [5, 6, 11, 27]. Our approach is aligned with this line of work but uses synthetic layouts instead of images as input. This is because semantic layouts are more abstract and, thus, more manipulable than images, which opens the door to many applications such as semantic editing, model validation, and domain adaptation.

III. METHODOLOGY

Problem Formulation. In SIS, our goal is to learn a mapping from a semantic label map, $m \in \mathcal{M}$ and a noise vector $z \in \mathcal{N}(0, 1)$ to a photorealistic RGB image, $x^R \in \mathcal{X}^R$. The labels m are one-hot encoded with C classes. In Synthetic-to-Real SIS, we exploit synthetic data from graphics engines and driving simulator to obtain images x^S and labels m^S in a cheap and automated fashion [17, 18], as the real images x^R are much more costly to annotate. Thus, we are given two datasets for training: a synthetic dataset, $\mathbf{D}^S = \{(x_i^S, m_i^S)\}_{i=1}^{N_S}$

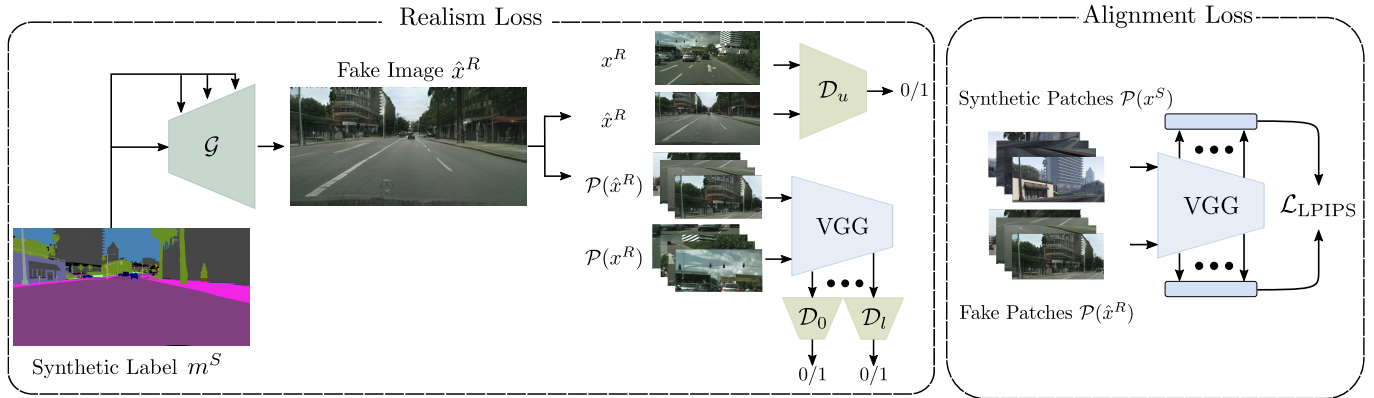


Fig. 3: An overview of the proposed unpaired framework. **Left:** We use a wavelet-based whole image discriminator and a discriminator ensemble in the high-level feature space to evaluate the realism of patches. **Right:** We use the synthetic image as a guide to promote better alignment with the semantic layout on a patch-level.

and a real dataset, $\mathbf{D}^R = \{x_j^R\}_{j=1}^{N_R}$. A model is trained to map a label m^S to an image x^R . Note that, unlike I2I models, we do not use synthetic images x^S as input. Conditioning the model on semantic layouts only allows maintaining easy controllability over scene generation, which is the goal of SIS [3, 21]. The output of the generator can be expressed as: $\hat{x}^R = \mathcal{G}(m, z)$.

A. Effect of semantic mismatch on model performance

Since these two datasets are collected independently, there exist discrepancies in the class distribution. For instance, \mathbf{D}^R can have more trees, while \mathbf{D}^S can have more buildings. As the labels for real images, m^R , are absent during training, we do not have an *a priori* knowledge of the class distribution of \mathcal{X}^R . To study the effect of cross-domain differences on generative models, we train 2 state-of-the-art models, CUT [11] and SRC [14], on the Synthetic-to-Real task. We use GTA-V [18] and Cityscapes [28] as the source and target domains. Results show that many semantic inconsistencies, such as generating trees or buildings instead of sky, appear in the generated images. Looking at the Cityscapes dataset shows that, in fact, the class 'sky' occupies a small part of the image on average, while this is not the case in GTA-V. This would suggest that previous works learn to sometimes ignore the semantic layout instead to better approximate the target domain distribution.

Overview of the proposed framework. Motivated by these findings, we present a framework named to bypass cross-domain differences. The framework trains a generator \mathcal{G} to satisfy two objectives: realism and alignment. Realism means that the generated images should have the appearance and texture of real images x^R , while the alignment objective states that the image should be aligned to the input semantic layout (see Figure 3). In the following, we describe how we accomplish the 2 objectives for the challenging use case of synthetic to real SIS.

B. Realism Objective

In previous works on unpaired GANs [5, 11–14], a discriminator is used to increase the realism of generated images.

An important design element in discriminators is its visual receptive field: what should the discriminator look at in the generated and real images to judge their realism? In previous works, there have been two different answers to this question: patch discrimination and whole image discrimination. The first approach outputs a matrix of realism scores, while the latter outputs only one score per image. In I2I, many works [5–7, 11, 12, 14, 27] used a patch discriminator [20] that judges the quality of individual image patches. On the other hand, it has been shown that whole image discrimination is more suitable for *under-constrained* conditional GANs like SIS [16]. Under-constrained means that the output image contains more details than the input layout. In this case, the discriminator needs to look at a larger spatial context to give stronger feedback to the generator.

However, both strategies become suboptimal in unpaired SIS when the distribution of \mathcal{X}^R is different than \mathcal{M}^S . We find that the whole image discriminator of USIS focuses on a small subset of visual cues that characterizes the distribution of \mathcal{X}^R . For instance, the discriminator might observe that \mathcal{X}^R contains a lot of trees and thus would push the generator to generate images with many trees, regardless of the input layout. This creates a semantic mismatch between the label and generated image, which is undesirable. On the other hand, we still observe that the patch discriminator does not encourage the generation of images with realistic texture. Instead, it is desirable that the discriminator learns the appearance or texture of the real images, not their semantic content, which should be determined by the input semantic map.

To overcome the shortcomings of both approaches, we draw inspiration from how a human would qualitatively judge the realism of an image. A human would first glance at the overall image and intuitively feel whether it is real or fake. Then, the human would closely inspect details of different scales, starting from more obvious and larger ones to smaller ones, to judge their quality. To realize this strategy, we first use a wavelet-based unconditional discriminator [16, 29], which we denote by \mathcal{D}_u to evaluate the realism of the generated

images. Then, we employ a discriminator ensemble, $\{\mathcal{D}_l\}_{l=1}^L$, to evaluate the realism of feature maps extracted from a pre-trained VGG network [30], which is frozen during training. Each discriminator processes its input feature map to a one-channel tensor featuring a realism score for each pixel. We use one discriminator on each of the last L ReLu layers of VGG. Each discriminator contains 5 layers consisting of (convolution-group normalization-ReLu). We use spectral normalization on all discriminators \mathcal{D}_l of the high-feature space and R1 regularization on the whole-image discriminator [31].

Discriminating high-level features has been used in previous works [27, 32] to focus on semantics instead of low-level details. While our work shares the same discriminator design as EPE [27], it differs in the regularization method. Specifically, instead of adding 1×1 convolution like [32], or using the adaptive backpropagation of [27], we regularize the discriminators by changing the input to the VGG extractor from the whole image to a stack of patches of the image. We define \mathcal{P} as the patch operator of the image x , which divides it into 4 patches with equal areas and stacks them along the batch dimension of the tensor. We define $\phi_l(x) = \text{VGG}_l(\mathcal{P}(x))$, as the feature of the l -th layer of the VGG network resulting from $\mathcal{P}(x)$. We argue that by providing smaller patches of the image, the VGG features are more fine-grained and more descriptive, because they depict a fewer number of objects than the entire image. This allows the discriminator ensemble to focus on more varied features, so it does not overfit the features of frequent and/or large classes. The adversarial learning objectives for the discriminators are:

$$\begin{aligned} \mathcal{L}_{adv_{D_l}} &= -\mathbb{E}_{x^R} \left[\log(\mathcal{D}_l(\phi_l(x^R))) \right] - \mathbb{E}_{m^S} \left[\log(1 - \mathcal{D}_l(\phi_l(\hat{x}^R))) \right], \\ \mathcal{L}_{adv_{D_0}} &= -\mathbb{E}_{x^R} \left[\log(\mathcal{D}_u(x^R)) \right] - \mathbb{E}_{m^S} \left[\log(1 - \mathcal{D}_u(\hat{x}^R)) \right]. \end{aligned} \quad (1)$$

The generator's adversarial loss becomes:

$$\mathcal{L}_{adv_G} = -\mathbb{E}_{m^S} \left[\log(\mathcal{D}_u(\hat{x}^R)) + \sum_{l=1}^L \log(\mathcal{D}_l(\phi_l(\hat{x}^R))) \right]. \quad (2)$$

We summarize our technical contributions in this part as follows:

- Unlike multi-scale discriminators in previous I2I applications [19, 33], which only consider patches of different resolutions, we employ a council of discriminators for the whole image and each of its patches simultaneously.
- Different than [27, 32], we provide regularization for the high-level feature discriminators by reducing the input to the VGG network though the defined operator \mathcal{P} .

C. Alignment Objective

In SIS, it is necessary to preserve the faithfulness of the generated image to the semantic layout. In our previous work, USIS [16], this objective was achieved through a U-Net [34] segmentation network \mathcal{S} that learns to segment the generated image into its input layout. However, when a domain shift is introduced between source and target domains, the cycle

segmentation loss becomes weaker than the adversarial loss, leading to deterioration in the mIoU score (see Table VI).

Our key idea to remedy this issue is to rely on the synthetic image x^S as a conditional guide for the generated image. Most importantly, we only wish to transfer the content of x^S to \hat{x}^R , not its texture. To this end, we use a perceptual loss, aka LPIPS loss, between \hat{x}^R and x^S . LPIPS has been extensively used [35, 36] to penalize structural differences between a generated and a reference image. It computes the similarity between the VGG features extracted from the 2 images.

Applying LPIPS loss between x^S and \hat{x}^R instead of the cycle segmentation loss of USIS leads to an improvement in the alignment score. However, we find that the alignment loss might often ignore small objects in the image. As a remedy, we propose to employ perceptual loss on a patch level instead of the global level. The alignment objective then becomes:

$$\mathcal{L}_{LPIPS} = \sum_l (\phi_l(\mathcal{P}(x^S)) - \phi_l(\mathcal{P}(\hat{x}^R)))^2, \quad (3)$$

where ϕ_l is the activation of the patches of the image from layer l in the VGG-network. Our motivation for applying a patchwise LPIPS is to amplify the alignment loss for smaller classes. A small object in an image would have a negligible contribution in the high-level representation of the whole image but would have a bigger contribution in the high-level representation of only a local part of that image.

IV. EXPERIMENTS

Datasets. We establish 2 benchmarks using 3 datasets: Cityscapes [28], GTA-V [18] and Mapillary [37]. In the first benchmark, GTA-V \rightarrow Cityscapes, we use 2 training sets: GTA-V labels and Cityscapes images. In the second benchmark, we use GTA-V labels and Mapillary images. Cityscapes contains street scenes in German cities with pixel-level annotations, while Mapillary contains more diverse street scenes around the world. GTA-V is a dataset containing 25k synthetic annotated images extracted from a computer game. For all 3 datasets, we use only the 34 classes defined by Cityscapes. For both experiments, we use the same image resolution (256×512) as USIS [15]. We use the last 5k images in the GTA-V dataset as a test split. We use a batchsize of 2, and a learning rate is 0.0001 in all experiments.

Metrics. A good generative model should generalize well on both synthetic and real labels, meaning it should perform well, whether the input to the model is a synthetic map m^S , or a real map, m^R . We use the Frechet Inception Distance (FID) and Kernel Inception Distance (KID) to measure image fidelity and mean Intersection over Union to measure the alignment between the generated images and the input labels. For mIoU calculation, a DRN-D-105 [38] pre-trained on the corresponding real dataset is used. We perform 2 sets of experiments: in the first, we train using GTA-V labels and Cityscapes images, and in the second, we use GTA-V labels and Mapillary images. To test the performance of each set of experiments, we use two test splits: 1) the first test split consists of the labels and images in the official validation splits

Method	GTA-V \rightarrow Cityscapes			Cityscapes Val. Split			GTA-V \rightarrow Mapillary			Mapillary Val. Split		
	FID \downarrow	mIoU \uparrow	KID \downarrow	FID \downarrow	mIoU \uparrow		FID \downarrow	mIoU \uparrow	KID \downarrow	FID \downarrow	mIoU \uparrow	
CUT [11]	66.6	21.0	0.029	75.4	29.6		66.5	6.0	0.047	73.4	16.4	
SRUnit [12]	67.7	16.7	0.028	82.1	23.4		67.4	9.2	0.042	70.8	16.5	
F-SeSim [13]	73.3	15.9	0.031	111.1	24.4		133.4	8.9	0.130	92.9	15.5	
SRC [14]	70.9	16.7	0.035	78.6	26.0		96.4	5.9	0.080	106.6	10.4	
USIS [15]	42.2	19.2	0.010	54.5	28.3		48.2	9.7	0.020	40.8	16.2	
Ours	40.4	27.1	0.012	67.3	40.6		46.2	15.5	0.023	44.2	24.0	

TABLE II: Comparison against SOTA methods on two benchmarks. Best results are denoted in red, while second best are denoted in blue.

Config	Generated Output during training	Alignment method	FID \downarrow	mIoU \uparrow	KID \downarrow
A	Whole Image	LPIPS on image level	60.5	21.8	0.0265
B	Whole Image	LPIPS on patch-level (4)	40.4	27.1	0.0120
C	Whole Image	LPIPS on patch-level (16)	55.1	24.9	0.0181
D	Individual Patches	LPIPS on patch level	102.4	19.4	0.0641

TABLE III: Comparison between different alignment strategies.

of the corresponding real dataset (Cityscapes/Mapillary), 2) the second test split consists of GTA-V labels in the test split (last $5k$ labels in the GTA-V dataset) and all images in the validation split of the real dataset. mIoU is always computed between the generated images and input labels, while FID is computed between the generated images and the images in the test split. In the tables, we denote test split 1 by the corresponding real dataset’s name and test split 2 by GTA-V \rightarrow Cityscapes/Mapillary.

V. RESULTS

A. Comparison against state-of-the-art

We compare against state-of-the-art unpaired generative models [11–15]. Our method is able to outperform existing methods in alignment in all settings by a large margin and is the best or second best in terms of image quality (FID, KID). We also notice that the proposed approach generalizes well when the input is a label from the real dataset (see Results on Cityscapes and Mapillary Val. splits). We show qualitative results on Cityscapes and Mapillary in Figure 4.

B. Ablation Studies

How to preserve alignment with the input label? In Table III, we compare between different alignment strategies. In Config A, we perform LPIPS on the whole image instead of patches; in Config B and C, LPIPS is performed on $\mathcal{P}(x)$ with 4 and 16 patches, respectively. All patches in the same experiment have equal size, i.e., in experiment B, patches have an area of 25% of the total image’s area. In Config D, we try a different approach: instead of generating whole images and aligning individual patches, we generate and align individual patches. In this setting, the training is done only on the patch level, which takes a substantially longer time to train. Results show that the hybrid approach of generating images and aligning patches is more optimal than generating and aligning images only or patches only. We find that the

patch size is also a very important design parameter; very small patches do not provide enough context for alignment.

Config	\mathcal{D}_u	$\{\mathcal{D}_l\}_{l=1}^L$	FID \downarrow	mIoU \uparrow	KID \downarrow
A	Patches (4)	Patches (4)	60.7	24.6	0.026
B	Patches (4)	Whole Image	72.8	20.6	0.030
C	Whole Image	Whole Image	51.8	21.4	0.018
D	Whole Image	Patches (16)	57.8	26.3	0.023
E	Whole Image	Patches (4)	40.4	27.1	0.012

TABLE IV: Comparison between different image discrimination strategies.

Method	GTA-V \rightarrow Cityscapes			Cityscapes Val. Split	
	FID \downarrow	mIoU \uparrow	KID \downarrow	FID \downarrow	mIoU \uparrow
Proposed Method	40.4	27.1	0.012	67.3	40.6
Two-Stage method	81.1	40.4	0.044	113.8	45.2

TABLE V: How to use the synthetic image as an intermediary for generating a photorealistic image? Comparison of our method with a simple alternative.

Which discrimination strategy to use? In Table IV, we compare different choices for image discrimination. In Config A, we present whole images to the wavelet-based discriminator \mathcal{D}_u and to the discriminator ensemble $\{\mathcal{D}_l\}_{l=1}^L$. In Config B, we present only patches as input to both discriminators, while in Config C and D, we experiment with hybrid approaches. Interestingly, whole image discrimination only (Config A) leads to a smaller FID and KID than Config B and C, but it demonstrates the poorest alignment. Config C and D achieve high alignment scores, but again a larger patch size proves to be essential for better diversity and alignment.

How to use the synthetic image as an intermediary for generating a photorealistic image? A key idea of our approach is to use the synthetic image as a guide to the content in the generated image because it can provide helpful spatial information not present in the input label map (edges and corners, boundaries between different objects, shadows, texture). We have used the synthetic image in the

Method	Dataset(s)	Mapillary		Cityscapes	
		FID ↓	mIoU↑	FID ↓	mIoU↑
CUT [11]	Single Domain	49.8	20.3	57.3	29.8
	Cross Domain	73.4	16.5	75.4	29.6
SRUnit [12]	Single Domain	54.8	16.7	74.8	21.8
	Cross Domain	70.8	16.5	82.1	23.4
F-SeSim [13]	Single Domain	74.1	21.1	76.9	23.0
	Cross Domain	92.9	15.5	111.1	24.4
SRC [14]	Single Domain	97.0	17.6	64.2	31.2
	Cross Domain	106.6	10.4	78.6	31.2
USIS [15]	Single Domain	23.8	31.0	53.7	44.8
	Cross Domain	54.6	14.8	54.5	28.3
Ours	Cross Domain	44.2	24.0	67.3	40.6

TABLE VI: Performance of different methods when trained in ideal conditions vs. when trained in a true unpaired setting. We show the strong performance of our model, trained on Cross Domain. The best results are marked in red; the second best are marked in blue.

alignment loss through a perceptual loss function. However, a very straightforward method to exploit the label map, is to learn the mapping between synthetic labels and images in a supervised way, then learn the mapping between the generated synthetic images and real images, using unpaired I2I model. In this “two-stage” approach, we employ OASIS [25] as the supervised SIS model and VSAIT [39] as the unpaired Synthetic-to-Real I2I model. Results in Table V reveal that while the alignment of this simple two-stage approach is better than our model, the FID is very high. Moreover, it doesn’t generalize well to real labels, as the FID remains very high, and the difference in mIoU is reduced, which justifies our approach.

On the utility of the proposed approach and task We compare the performance of our model against the state-of-the-art trained on the Synthetic-to-Real dataset and on the Real dataset only in an unpaired manner. We report the performance on the validation split of Mapillary. Results show that the performance of previous works substantially drops when their training and test distributions differ. However, the proposed approach achieves high image fidelity and strong alignment on the real labels in test-time, although they were unseen during training. More interestingly, the performance of our model surpasses 4 state-of-the-art models trained on the original dataset and comes only second to USIS. This implies that a carefully designed generative model trained on synthetic data can generalize well to real data.

VI. CONCLUSION

In this work, we explore a new task that exploits synthetic data to train a generative model for SIS, substantially alleviating labeling costs without sacrificing photorealism. Compared to synthetic-to-real I2I, this task has the advantage of allowing easier manipulation in the image space post-generation. We presented a framework that outperforms previous works on this task and has interestingly shown a strong generalization ability when the test-time input labels are drawn from a different distribution than the labels seen during training. Most importantly, we have shown that a hybrid approach of discriminating

both images and patches is key to bypassing the semantic domain gap between images and labels. Additionally, using the synthetic image as a guide to a patch content loss promotes stronger alignment without undermining the photorealism of generated images. We believe that the proposed task can offer a pragmatic setting for training generative models and encourage future works to explore how to use synthetic data to train generative models for stronger generalization.

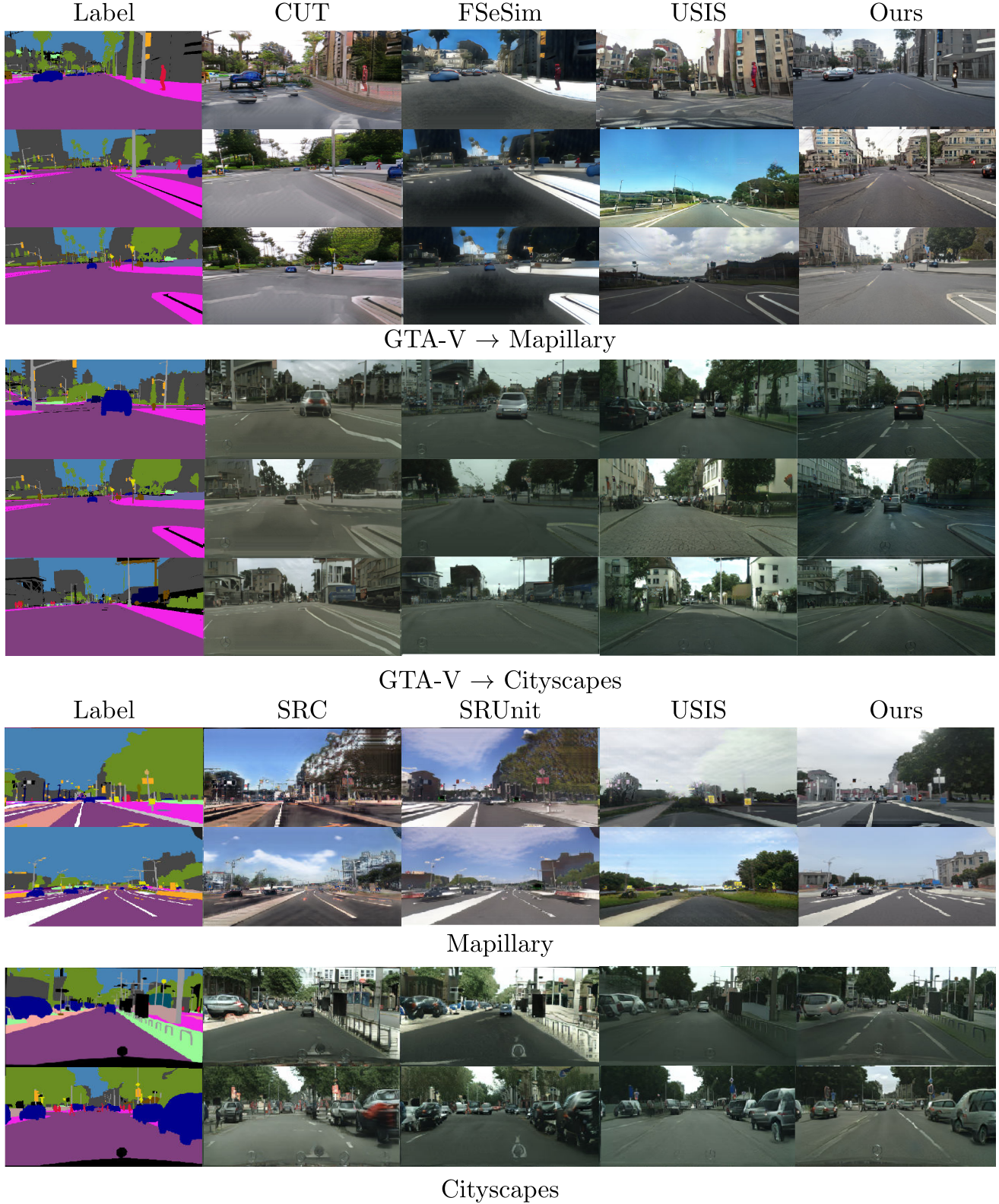


Fig. 4: We show qualitative results for our model and other baselines on GTA-V \rightarrow Mapillary, GTA-V \rightarrow Cityscapes, Mapillary, Cityscapes

REFERENCES

[1] Éloi Zablocki et al. “Explainability of deep vision-based autonomous driving systems: Review and challenges”. In: *International Journal of Computer Vision* (2022), pp. 1–28.

[2] Guillaume Le Moing et al. “Semantic Palette: Guiding Scene Generation with Class Proportions”. In: *Proceedings of the IEEE/CVF Conference on Computer Vision and Pattern Recognition*. 2021, pp. 9342–9350.

[3] Samaneh Azadi et al. “Semantic bottleneck scene generation”. In: *arXiv preprint arXiv:1911.11357* (2019).

[4] Anna Volokitin, Ender Konukoglu, and Luc Van Gool. “Decomposing image generation into layout prediction and conditional synthesis”. In: *Proceedings of the IEEE/CVF Conference on Computer Vision and Pattern Recognition Workshops*. 2020, pp. 372–373.

[5] Jun-Yan Zhu et al. “Unpaired image-to-image translation using cycle-consistent adversarial networks”. In: *International Conference on Computer Vision (ICCV)*. 2017.

[6] Xun Huang et al. “Multimodal unsupervised image-to-image translation”. In: *European Conference on Computer Vision (ECCV)*. 2018.

[7] Hsin-Ying Lee et al. “Diverse Image-to-Image Translation via Disentangled Representation”. In: *European Conference on Computer Vision (ECCV)*. 2018.

[8] Matthew Amadio and Smita Krishnaswamy. “Travelgan: Image-to-image translation by transformation vector learning”. In: *Proceedings of the IEEE Conference on Computer Vision and Pattern Recognition*. 2019, pp. 8983–8992.

[9] Sagie Benaim and Lior Wolf. “One-sided unsupervised domain mapping”. In: *Advances in Neural Information Processing Systems (NeurIPS)*. 2017.

[10] Huan Fu et al. “Geometry-consistent generative adversarial networks for one-sided unsupervised domain mapping”. In: *Conference on Computer Vision and Pattern Recognition (CVPR)*. 2019.

[11] Taesung Park et al. “Contrastive Learning for Unpaired Image-to-Image Translation”. In: *European Conference on Computer Vision*. 2020.

[12] Zhiwei Jia et al. “Semantically robust unpaired image translation for data with unmatched semantics statistics”. In: *Proceedings of the IEEE/CVF International Conference on Computer Vision*. 2021, pp. 14273–14283.

[13] Chuanxia Zheng, Tat-Jen Cham, and Jianfei Cai. “The spatially-correlative loss for various image translation tasks”. In: *Proceedings of the IEEE/CVF Conference on Computer Vision and Pattern Recognition*. 2021, pp. 16407–16417.

[14] Chanyong Jung, Gihyun Kwon, and Jong Chul Ye. “Exploring Patch-wise Semantic Relation for Contrastive Learning in Image-to-Image Translation Tasks”. In: *Proceedings of the IEEE/CVF Conference on Computer Vision and Pattern Recognition*. 2022, pp. 18260–18269.

[15] George Eskandar et al. “Wavelet-Based Unsupervised Label-to-Image Translation”. In: *ICASSP 2022 - 2022 IEEE International Conference on Acoustics, Speech and Signal Processing (ICASSP)*. 2022, pp. 1760–1764. DOI: [10.1109/ICASSP43922.2022.9746759](https://doi.org/10.1109/ICASSP43922.2022.9746759).

[16] George Eskandar et al. “USIS: Unsupervised Semantic Image Synthesis”. In: *Computers & Graphics* (2023). ISSN: 0097-8493. DOI: <https://doi.org/10.1016/j.cag.2022.12.010>. URL: <https://www.sciencedirect.com/science/article/pii/S0097849323000018>.

[17] Alexey Dosovitskiy et al. “CARLA: An open urban driving simulator”. In: *Conference on robot learning*. PMLR. 2017, pp. 1–16.

[18] Stephan R. Richter et al. “Playing for Data: Ground Truth from Computer Games”. In: *European Conference on Computer Vision (ECCV)*. Ed. by Bastian Leibe et al. Vol. 9906. LNCS. Springer International Publishing, 2016, pp. 102–118.

[19] Ting-Chun Wang et al. “High-resolution image synthesis and semantic manipulation with conditional GANs”. In: *Conference on Computer Vision and Pattern Recognition (CVPR)*. 2018.

[20] Phillip Isola et al. “Image-to-image translation with conditional adversarial networks”. In: *Conference on Computer Vision and Pattern Recognition (CVPR)*. 2017.

[21] Taesung Park et al. “Semantic image synthesis with spatially-adaptive normalization”. In: *Conference on Computer Vision and Pattern Recognition (CVPR)*. 2019.

[22] Zhentao Tan et al. “Rethinking Spatially-Adaptive Normalization”. In: *arXiv:2004.02867* (2020).

[23] Peihao Zhu et al. “SEAN: Image Synthesis With Semantic Region-Adaptive Normalization”. In: *2020 IEEE/CVF Conference on Computer Vision and Pattern Recognition (CVPR)* (2020), pp. 5103–5112.

[24] Xihui Liu et al. “Learning to predict layout-to-image conditional convolutions for semantic image synthesis”. In: *Advances in Neural Information Processing Systems (NeurIPS)*. 2019.

[25] Edgar Schönfeld et al. “You Only Need Adversarial Supervision for Semantic Image Synthesis”. In: *International Conference on Learning Representations*. 2021.

[26] Hao Tang et al. “Edge guided GANs with semantic preserving for semantic image synthesis”. In: *arXiv preprint arXiv:2003.13898* (2020).

[27] Stephan R Richter, Hassan Abu Alhaija, and Vladlen Koltun. “Enhancing photorealism enhancement”. In: *IEEE Transactions on Pattern Analysis & Machine Intelligence* 45.02 (2023), pp. 1700–1715.

[28] Marius Cordts et al. “The cityscapes dataset for semantic urban scene understanding”. In: *Conference on Computer Vision and Pattern Recognition (CVPR)*. 2016.

[29] Rinon Gal et al. “SWAGAN: A Style-based Wavelet-driven Generative Model”. In: *ArXiv abs/2102.06108* (2021).

[30] Karen Simonyan and Andrew Zisserman. “Very deep convolutional networks for large-scale image recognition”. In: *arXiv preprint arXiv:1409.1556* (2014).

[31] Tero Karras, S. Laine, and Timo Aila. “A Style-Based Generator Architecture for Generative Adversarial Networks”. In: *2019 IEEE/CVF Conference on Computer Vision and Pattern Recognition (CVPR)* (2019), pp. 4396–4405.

[32] Axel Sauer et al. “Projected gans converge faster”. In: *Advances in Neural Information Processing Systems* 34 (2021), pp. 17480–17492.

[33] Satoshi Iizuka, Edgar Simo-Serra, and Hiroshi Ishikawa. “Globally and locally consistent image completion”. In: *ACM Transactions on Graphics (ToG)* 36.4 (2017), pp. 1–14.

[34] O. Ronneberger, P. Fischer, and T. Brox. “U-Net: Convolutional Networks for Biomedical Image Segmentation”. In: *MICCAI*. 2015.

[35] L. A. Gatys, A. S. Ecker, and M. Bethge. “Image Style Transfer Using Convolutional Neural Networks”. In: *Conference on Computer Vision and Pattern Recognition (CVPR)*. 2016.

[36] Alexey Dosovitskiy and Thomas Brox. “Generating Images with Perceptual Similarity Metrics based on Deep Networks”. In: *Advances in Neural Information Processing Systems (NeurIPS)*. Ed. by D. D. Lee et al. 2016.

[37] Gerhard Neuhold et al. “The mapillary vistas dataset for semantic understanding of street scenes”. In: *Proceedings of the IEEE international conference on computer vision*. 2017, pp. 4990–4999.

[38] Fisher Yu, Vladlen Koltun, and Thomas Funkhouser. “Dilated residual networks”. In: *Conference on Computer Vision and Pattern Recognition (CVPR)*. 2017.

[39] Justin Theiss et al. “Unpaired Image Translation via Vector Symbolic Architectures”. In: *Computer Vision–ECCV 2022: 17th European Conference, Tel Aviv, Israel, October 23–27, 2022, Proceedings, Part XXI*. Springer. 2022, pp. 17–32.